Free Radical Biology and Medicine 53 (2012) 1595–1606

Contents lists available at SciVerse ScienceDirect

Free Radical Biology and Medicine

journal homepage: www.elsevier.com/locate/freeradbiomed

Original Contributions

Zinc supplementation prevents cardiomyocyte apoptosis and congenital heart defects in embryos of diabetic mice

Srinivasan Dinesh Kumar [a,b,*], Murugaiyan Vijaya [a], Ramar Perumal Samy [a], S. Thameem Dheen [a], Minqin Ren [c], Frank Watt [c], Y. James Kang [d,e], Boon-Huat Bay [a], Samuel Sam Wah Tay [a,*]

[a] Department of Anatomy, National University Health System, National University of Singapore, Singapore 117597
[b] Lee Kong Chian School of Medicine, Nanyang Technological University, 50 Nanyang Drive, Singapore 637553
[c] Centre for Ion Beam Applications, Department of Physics, Faculty of Science, National University of Singapore, Singapore 117542
[d] Department of Medicine, University of Louisville School of Medicine, Louisville, KY 40292, USA
[e] Regenerative Medicine Research Center, Sichuan University West China Hospital, Sichuan, China

ARTICLE INFO

Article history:
Received 16 November 2011
Received in revised form
2 July 2012
Accepted 8 July 2012
Available online 20 July 2012

Keywords:
Cardiac malformations
Maternal diabetes
Oxidative stress
Antioxidant
Zinc
Metallothionein
Nuclear microscopy
Heart
Embryos
Mice

ABSTRACT

Oxidative stress induced by maternal diabetes plays an important role in the development of cardiac malformations. Zinc (Zn) supplementation of animals and humans has been shown to ameliorate oxidative stress induced by diabetic cardiomyopathy. However, the role of Zn in the prevention of oxidative stress induced by diabetic cardiac embryopathy remains unknown. We analyzed the preventive role of Zn in diabetic cardiac embryopathy by both in vivo and in vitro studies. In vivo study revealed a significant decrease in lipid peroxidation, superoxide ions, and oxidized glutathione and an increase in reduced glutathione, nitric oxide, and superoxide dismutase in the developing heart at embryonic days (E) 13.5 and 15.5 in the Zn-supplemented diabetic group when compared to the diabetic group. In addition, significantly down-regulated protein and mRNA expression of metallothionein (MT) in the developing heart of embryos from diabetic group was rescued by Zn supplement. Further, the nuclear microscopy results showed that trace elements such as phosphorus, calcium, and Zn levels were significantly increased ($P < 0.001$), whereas the iron level was significantly decreased ($P < 0.05$) in the developing heart of embryos from the Zn-supplemented diabetic group. In vitro study showed a significant increase in cellular apoptosis and the generation of reactive oxygen species (ROS) in H9c2 (rat embryonic cardiomyoblast) cells exposed to high glucose concentrations. Supplementation with Zn significantly decreased apoptosis and reduced the levels of ROS. In summary, oxidative stress induced by maternal diabetes could play a role in the development and progression of cardiac embryopathy, and Zn supplementation could be a potential therapy for diabetic cardiac embryopathy.

Introduction

Maternal diabetes has been shown to affect early organogenesis, leading to congenital malformations in various organ systems including the heart [1,2]. Our recent studies revealed that maternal diabetes causes massive cell damage, increase in apoptosis, decrease in proliferation index, and defective heart development in mouse embryos [3,4]. Hyperglycemia causes the cellular oxidative damage by increasing production of ketone bodies, which lead to generation of reactive oxygen species (ROS). The increased level of ROS causes the free radical generation and decreased antioxidants or both [5], which eventually influence the organogenesis during development. Therefore, an efficient antioxidant system including superoxide dismutase (SOD), catalase, glutathione peroxidase (Gpx), reduced glutathione (GSH), and α-tocopherol is critical to the well-being the heart [6]. Zinc (Zn) is known to participate in various cellular functions. It has an antioxidant action in protecting the adult heart from various oxidative stresses. Its abnormal metabolism is related to certain disorders including diabetic complications [7].

In addition to Zn and other antioxidant systems, metallothionein (MT) plays a key role in the scavenging of free radicals. The role of MT as an antioxidant has been extensively studied [8–10]. Zn and its involvement in the synthesis of the antioxidant MT have attracted much attention in diabetes research [11,12].

Abbreviations: EC, endocardial cushion; OFT, outflow tract; NO, nitric oxide; ROS, reactive oxygen species; SOD, superoxide dismutase; TBARS, thiobarbituric acid-reactive substance; MDA, malondialdehyde; GPx, glutathione peroxidase; GSH, reduced glutathione; GSSG, oxidized glutathione; P, phosphorus; Ca, calcium; Fe, iron; Zn, zinc; Cu, copper; Mn, manganese; Mg, magnesium; Se, selenium; STZ, streptozotocin; MT, metallothionein; H9c2 cells, rat embryonic cardiomyoblasts

* Corresponding authors. Fax: +65 67787643.
E-mail addresses: dineshkumar@ntu.edu.sg (S.D. Kumar), anttaysw@nus.edu.sg (S.S.W. Tay).

0891-5849/$ - see front matter © 2012 Elsevier Inc. All rights reserved.
http://dx.doi.org/10.1016/j.freeradbiomed.2012.07.008

Maternal diabetes causes a significant systemic oxidative stress and is often accompanied by Zn deficiency that increases the susceptibility of the embryonic heart to oxidative damage. Therefore, there is a strong rationale to consider Zn supplementation as the therapeutic strategy to prevent or reduce oxidative damage in diabetic cardiac embryopathy.

Nuclear microscopy techniques have the ability to image density variations in relatively thick tissue, map trace elements at the cellular level, and extract quantitative information on these elements [13]. Several groups have shown that some trace elements [such as Zn, copper (Cu), manganese (Mn), and selenium (Se) as cofactors of antioxidant enzymes] play a major role in protecting the insulin-secreting pancreatic beta cells, which are sensitive to free radical damage [14,15]. In addition, the trace element Zn might have an antidiabetic effect by decreasing iron (Fe) levels in the lesion, possibly leading to the inhibition of iron-catalyzed free radical reactions.

The main aim of this study was to understand the oxidative change in the developing heart of embryos from Zn-supplemented diabetic mice, as well as the cellular damage induced by glucose-dependent oxidative stress and the protective role of Zn on H9c2 (embryonic rat cardiomyoblast) cells. Taken together, these results provide further insight into the role of Zn in the prevention of diabetes-induced congenital heart defects, which may give rise to the development of effective treatments against diabetic cardiac embryopathy.

Materials and methods

Animals

The Swiss Albino mice used in the present study were obtained from the Laboratory Animals Centre, Singapore. All procedures involving animals handling was in accordance with Principles of Laboratory Animal Care (NIH publication No. 85-23, revised 1985) and guidelines of the Institutional Animal Care and Use Committee (IACUC), National University of Singapore.

Induction of diabetes mellitus and Zn supplementation

Diabetes mellitus was induced in 8-week-old female mice by an intraperitoneal injection of streptozotocin for three successive days (STZ, 75 mg/kg body weight, Sigma, USA) dissolved in citrate buffer (0.01 M, pH 4.5). Blood glucose level was examined 1 week after STZ injection using Glucometer Elite (Bayer, USA). Mice with nonfasting blood glucose levels exceeding 16 mmol/L were used as diabetic mice. In contrast, control mice maintained the normal blood glucose levels (4–6 mmol/L) before and during pregnancy. Timed mating was carried out by placing four female mice with one normal male mouse in a cage overnight. The day when a copulation plug was observed was counted as embryonic day 0.5 (E0.5). For Zn supplementation diabetic group, Zn sulfate (5 mg/kg body wt) was given intraperitoneally from E0.5 to E13.5 or E15.5 days. Time-mated pregnant mice were divided into three groups: (a) control, (b) diabetes, and (c) diabetes with Zn supplementation. At E13.5 and E15.5, pregnant mice were anesthetized with pentobarbital (150 mg/kg body wt, intraperitoneally) and embryos were collected via Caesarean section. For each experiment, hearts were isolated from embryos from the three groups at different time points. The developmental stage E13.5 corresponds to ~6 weeks of human gestation [16,17]; hence it was chosen as one of the time points. At this stage all 4 chambers of the heart were clearly distinguishable, and the outflow tract (OFT) was evident [18]. In addition, the heart phenotype was apparent in embryos of diabetic mice [3]. Malformed embryos from diabetic mice, normal embryos from diabetic and nondiabetic mice, and normal embryos from Zn-supplemented diabetic mice were used as the diabetic, control, and Zn-supplemented diabetic groups, respectively.

Nitric oxide assay

The total amount of nitric oxide in the heart samples was assessed by the Griess reaction with a colorimetric assay kit (U.S. Biological, Swampscott, MA) that detects nitrite (NO_2^-), a stable reaction product of nitric oxide. Hearts from the embryos of control, diabetic, and Zn-supplemented diabetic mice were collected and homogenized in homogenizing buffer (T-PER; Pierce Biotechnology, Inc., Rockford, IL). Homogenate was centrifuged at 14,000 *g* for 15 min, and the supernatant was collected for the assay. Briefly, 80 μl of samples was added with 10 μl of enzyme cofactor followed by 10 μl of nitrate reductase, according to the manufacturer's instructions, and incubated for 1 h at room temperature (26 °C). Griess reagents (50 μl) A and B were added to the above solution, and the color developed at room temperature after 10 min was measured. The optical density of each of the samples was recorded at 540 nm using a microplate reader (GENios, Tecan Austria GmbH, Grodig/Salzburg, Austria). The nitrite concentration (in μM) was determined from a nitrite standard curve.

Measurement of lipid peroxidation

Heart tissue was homogenized in RIPA homogenizing buffer. The level of lipid peroxidation was estimated by the thiobarbituric acid (TBA) test according to the method described by Ohkawa et al. [19]. Further, the artifactual lipid oxidation is prevented by using butylated hydrotoluene (BHT) during the sample collection. Homogenate was centrifuged at 1600 *g* for 10 min at 4 °C and the supernatant was used for the assay. The amount of 100 μl of supernatant from each sample was taken in a vial and 100 μl of SDS was added and vials were boiled in vigorously boiling water. After an hour, vials were removed and kept in ice bath for 10 min to stop the reaction. The vials were centrifuged at 1600 *g* at 4 °C. The optical density of 150 μl of sample was read at 530 nm using a microplate reader (GENios, Tecan Austria GmbH, Grodig/Salzburg, Austria). The malondialdehyde (MDA) concentration (in μM) was determined from a MDA standard curve.

Detection of superoxide anion

Accumulation of superoxide anion in the developing heart was quantified using a cytochrome reduction assay [20]. Tissue was homogenized and centrifuged at 800 *g*. The supernatant was incubated in the presence of 30 μM succinylated cytochrome *c* and 1 mM NADPH. The change in absorbance at 550 nm was measured. The difference in the amount of reduced succinylated cytochrome *c* in the presence or absence of 0.2 mg/ml superoxide dismutase was used to estimate the amount of superoxide anion by employing an absorbance coefficient 21.1 $M^{-1}\,cm^{-1}$.

Measurements for reduced and oxidized glutathione

A GSH/GSSG kit from U.S. Biological was used to measure reduced glutathione (GSH) and oxidized glutathione (GSSG). The heart tissue was homogenized in 6 vol of 5% metaphosphoric acid with or without 30 mM/L 1-methyl-2-vinyl pyridinium trifluoromethane sulfonate (M2VP), a scavenger of GSH. The homogenate was centrifuged at 1000 *g* for 5 min. For GSH estimation, 5 μl of supernatant was mixed with 355 μl assay buffer containing 100 mM/L sodium phosphate and 5 mM/L EDTA, pH 7.5. For GSSG estimation, 10 μl homogenate with M2VP was mixed with GSSG buffer containing 100 mM/L sodium phosphate and 5 mmol/L EDTA, pH 10.05.

The samples were mixed with 1.22 mM/L 5,5′-dithiobis-(2-nitrobenzoic acid) and 15 U/ml GSH reductase. The mixture was incubated at room temperature for 5 min, and the absorbance was recorded at 412 nm for 3 min after the addition of 3.8 μmol of NADPH.

Measurements of cytosolic and mitochondrial superoxide dismutase

The total amount of both cytosolic and mitochondrial superoxide dismutase (SOD) in the developing heart samples was assessed by the colorimetric assay kit (Cayman Chemicals, Ann Arbor, MI). Tissue was homogenized in 20 mM Hepes buffer, pH 7.2, containing 1 mM EGTA, 210 mM mannitol, and 70 mM sucrose per gram tissue. In order to assay the total SOD activity (cytosolic and mitochondrial SOD), two enzymes were separated by centrifuging the homogenate at 10,000 *g* for 15 min. The resultant 10,000 *g* supernatant contained cytosolic SOD and the pellet contained mitochondrial SOD. Mitochondrial pellet was homogenized in cold Hepes buffer. Radical detector was added to each sample and it was followed by xanthine oxidase to initiate the reaction. Samples were incubated for 20 min in an orbital shaker at room temperature. Absorbance was measured at 450 nm using a plate reader.

Quantitative real-time RT-PCR

Total RNA from developing hearts was extracted using RNeasy mini kit (Qiagen, Hilden, Germany). The reaction mixture containing 2 μg of RNA, 2.5 μM oligo(dT) primer, 200 U of Molony murine leukemia virus reverse transcriptase (MMLV, Promega, USA), 2 mM of each dNTPs, and 5 U of RNasin in a total volume of 25 μl was incubated for 1 h at 42 °C to synthesize cDNA. For real time RT-PCR, aliquots (5 μl) of cDNA products were amplified in the reaction mixture (20 μl) containing LightCycler FastStart DNA Master SYBR Green I, 0.5 μM of each primer in a LightCycler instrument (Roche Molecular Biochemicals, Germany) as instructed by the manufacturer. The primer used for MT-1 was 5′-ccaactgctcctgctccac-3′ 5′-cgcctttgcagacacagc-3′. The fold change of mRNA was analyzed by 2-ΔΔCt method [21].

Immunohistochemistry

As described previously [3], the cryosections were incubated with the primary MT antibody (1:50; Dako Corporation, Carpinteria, CA) in PBS containing 0.1% Triton X-100 (PBS-TX) at 4 °C overnight. Sections were then washed in PBS and incubated in the anti-mouse IgG (1:200; Sigma) for 1 h at RT. The sections were subsequently processed using an ABC kit (Vector Laboratories, Burlingame, CA, USA) for 1 h at RT, and reaction products were finally visualized using 3,3-diaminobenzidine tetrahydrochloride (DAB; Sigma, St. Louis, MO) as the substrate. Tissue sections were counterstained by 0.5% methyl green nuclear stain for 10 min, dehydrated by immersion in alcohol, and then cleared with xylene before mounting in medium (Permount; Fisher Scientific, Pittsburgh, PA). Control sections were incubated as described above but without the primary antibody. Photomicrographs were taken with a light microscope (Olympus BX51, Olympus, Japan).

Sample preparation for nuclear microscopy

Animals were sacrificed and heart samples from the embryos of control, diabetic, and Zn-supplemented diabetic mice were harvested. Serial sagittal sections of 20 μm thickness were cut (Leica CM 3050, Leica Microsystems, Nussloch, Germany) and picked up on freshly made thin organic pioloform film ($\sim$ 0.5 μm in thickness) mounted on nuclear microscopy targeted holders for subsequent nuclear microscopy measurements.

Nuclear microscopy analysis

The experiments were carried out using the 2.1 MeV proton beam focused to 1 μm spot size as calibrated by the Nuclear Microscopy facility at the Centre for Ion Beam Applications (CIBA), National University of Singapore, Singapore [13]. Scanning transmission ion microscopy (STIM) was used to position the area of interest on the sample studied prior to data acquisition which uses the combination of particle-induced X-ray emission (PIXE) technique and Rutherford backscattering spectrometry (RBS) for quantitative measurement of the trace elements present in the sample. PIXE is a well-established technique for trace elemental analysis offering nondestructive multielemental capability and low detection limits. It allows simultaneous detection of elements from Na onwards in the periodic table, with a sensitivity of about 1 ppm in biological materials such as tissue sections and cells [22]. The data obtained from RBS allow for matrix characterization and beam–sample interaction information in order for quantitative analysis. The strength of nuclear microscopy lies in its elemental mapping capability at the parts per million levels coupled with the ability to measure trace element concentrations at high quantitative accuracy independent of chemical state of the element [23].

Cell culture

The H9c2 cells were obtained from ATCC, USA. The cells were maintained at 37 °C in a humidified chamber with 5% CO_2 in 25 cm^2 cell culture flask containing Dulbecco's modified Eagle's medium (NUMI, NUS, Singapore) supplemented with 10% fetal bovine serum and 2 mM L-glutamine (Invitrogen, Carlsbad, CA). The cells were passaged when they reached 90% confluence by treatment with 0.25 mM trypsin and 0.03% EDTA (Invitrogen) and they were seeded at 10,000 cells/cm^2 for every experiment (ROS measurement and cell cycle analysis).

Reactive oxygen species assay

DCFH-DA is a cell-permeable compound. When the compound enters into the cell its acetate group is cleaved by cellular esterases and nonfluorescent DCFH is trapped inside. Subsequent oxidation by reactive oxygen species (ROS) of DCFH yields the fluorescent product DCF. Therefore DCFH-DA is an ROS-sensitive probe that can be used to detect oxidative activity in living cells. In this experiment, H9c2 cells were grown in 6-well plates for 48 h to reach 80% confluence. Then, the cells were exposed to 5.5 and 44 mM concentrations of glucose alone or in combination with Zn (5.5 and 44 mM) for 24 h in culture medium before introducing 60 μl of DCFH-DA for 30 min in an incubator at a final concentration of 10 μm/L. Data were collected by a flow cytometer (DakoCytomation, Denmark), equipped with a glass tube reader, at an excitation/emission wavelength of 485/530 nm. The intracellular ROS level was expressed by the ratio of fluorescence density over the quantity of protein [7].

Cell cycle analysis

The confluent H9c2 cells were washed with PBS and treated with trypsin (1000 U/ml) containing 5.3 mM EDTA for 3 min at 37 °C. The cell suspension was spun at 1000 *g* for 5 min at room temperature. Resuspended cells were seeded in 6-well microplates (Nalge Nunc International, USA) with an initial density 2.5×10^5 cells/well in culture medium. Briefly, cells were incubated with various glucose concentrations (5.5 and 44 mM) served as diabetic or in combination of Zn supplementation (5.5 and 44 mM) served as a treatment and cell without any treatment served as a normal control. The plates were incubated for 24 h at 37 °C in 5% CO_2 incubator. The trypsinized

cells were centrifuged at 1800 *g* for 5 min. The cell pellets were resuspended in 0.5 ml of PBS and 4.5 ml of 70% ice-cold ethanol and incubated at 4 °C for 24 h. The cells containing ice-cold ethanol were centrifuged at 1800 *g* for 5 min at 4 °C. The cell pellet was washed twice in PBS and 1 ml of cocktail (10 µl of 0.1% Triton-X in 4 mM sodium citrate, pH 7.8, 2 ml of 720 U/ml of RNAse and 200 µl of 100 µg/ml of propidium iodide) was added to the cell suspension to a final concentration of 2 million cells/ml incubated at 37 °C for 30 min. The proportion of cells in each phase of the cell cycle was determined with flow cytometry using a DakoCytomation flow cytometer equipped with Summit SW Version 4.3.02 software (Beckman Coulter, USA). The percentage of apoptotic cells was calculated as the percentage of the number of apoptotic cells over the total number of the cells [24]. The morphology was observed and images were captured under a light microscope connected with a digital camera (Nikon, Japan).

TUNEL assay

DNA fragmentation in situ was detected by means of the terminal deoxynucleotidyl transferase (TdT)-mediated 2-deoxyuridine 5-triphosphate (dUTP) nick-end labeling (TUNEL) assay, according to the kit instructions (Roche, Germany). Briefly, H9c2 cells were fixed with 4% paraformaldehyde in PBS for 1 h at room temperature, 13-mm coverslips (Marlenfeld GmbH Co, Germany) were rinsed with PBS for 5 min and incubated in a permeablization solution (1% Triton X-100 in 0.1% sodium citrate) for 2 min on ice, and the TUNEL reaction mixture was added for 1 h at 37 °C in a humidified atmosphere (5% CO_2) in the dark. Negative controls were set up by adding labeling solutions without terminal transferase instead of the TUNEL reaction mixture. After rinsing with PBS, samples were analyzed under a fluorescence microscope using an excitation wavelength in the range of 450–500 nm, and detection was in the range 515–565 nm [7].

Table 1
Number (mean ± SD) of embryos obtained from the control, diabetic, and Zn-supplemented diabetic mice.

	Control	Diabetic	Zn-supplemented diabetic
No. of animal studied	3	7	5
Total No. of embryos studied	32	52	46
No. of embryos per litter	10.67 ± 0.58	7.42 ± 0.98	9.2 ± 0.84**

** $P < 0.001$ diabetic vs Zn-supplemented diabetic.

Statistical analysis

The data are expressed as mean ± SD. Statistical software (Graphpad Prism 4.1, USA) was used. For tests of significance between two groups within multiple groups, one-way analysis of variance (ANOVA) and *t* test were performed. *P* value 0.05 was considered as statistically significant.

Results

In vivo studies

Maternal blood glucose levels of diabetic and Zn-supplemented diabetic groups were higher (> 16 mmol/L) than those of the control group (4–6 mmol/L). Embryos with malformations from diabetic mice and normal embryos from Zn-supplemented diabetic and nondiabetic control mice were used for this study. The total number of embryos per litter was significantly increased ($P < 0.001$) in the Zn-supplemented diabetic group (9.2 ± 0.84) when compared to the diabetic group (7.42 ± 0.98) (Table 1). Embryos from diabetic mice had congenital malformations such as neural tube defects (Fig. 1B) and the OFT defects (Fig. 1E). In contrast, the frequencies for cardiac and extracardiac malformations in the embryos appear to be decreased in the Zn-supplemented diabetic group (Figs. 1C and 1F) when compared to the diabetic group (Figs. 1B and 1E) (Table 2).

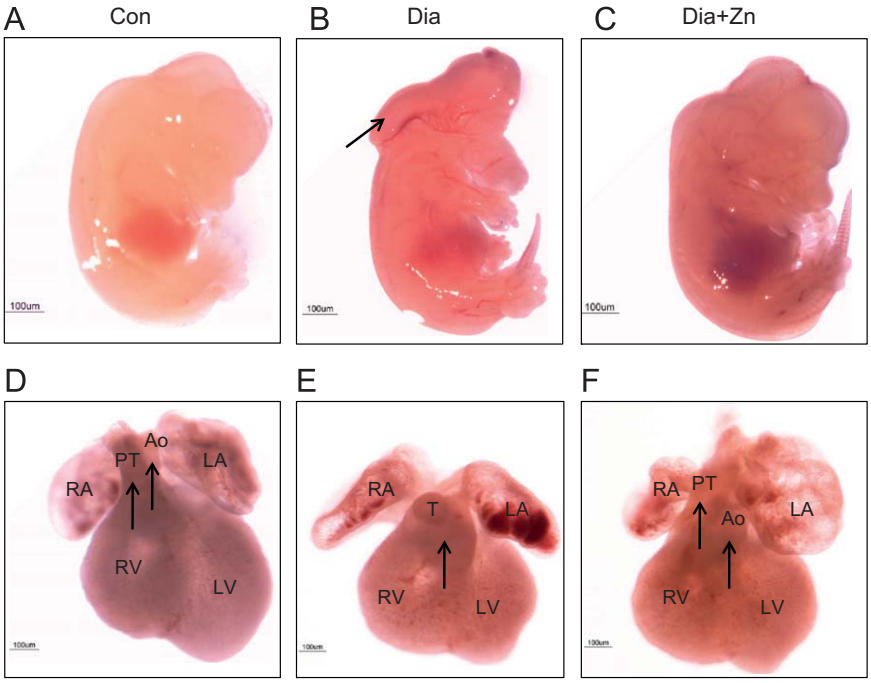

Fig. 1. Embryos obtained from control (A), diabetic (B), and Zn-supplemented diabetic (C) mice. In control and Zn-supplemented diabetic mice embryos, the Ao and PT have separated (arrows) and are connected to the LV and RV, respectively (connections verified by sectioning, data not shown) (D, F). Embryo from diabetic mice shows neural tube defect (arrow) (B). In addition, there is a single outflow vessel (arrow), which is wholly committed to the RV (E).

Superoxide concentration

In order to elucidate the changes in superoxide accumulation in the developing heart of embryos from the three groups, superoxide formation was quantified by SOD-inhabitable cytochrome *c* reduction assay. The cardiac superoxide concentration was significantly increased ($P<0.001$) in the diabetic group when compared to the control group in both time points (E13.5 and E15.5). In the Zn-supplemented diabetic group, the cardiac superoxide concentration was significantly reduced ($P<0.001$) when compared with the diabetic group (Fig. 2A).

Nitric oxide level

To investigate the possible mechanism responsible for the development of cardiac malformations in embryos from diabetic mice, nitric oxide (NO) levels in the developing heart at E13.5 and E15.5 were studied. The total amounts of NO in the developing heart from all groups were assessed calorimetrically (Fig. 2B). The total amounts of NO in the developing heart sample were significantly decreased ($P<0.05$) in embryos of diabetic group when compared with control and Zn-supplemented diabetic groups.

Table 2
Frequencies for cardiac and extracardiac malformations in the embryos from control, diabetic, and Zn-supplemented diabetic mice.

	Control ($n=32$)	Diabetic ($n=52$)	Zn-supplemented diabetic ($n=46$)
No. of embryos with cardiac malformations[a]	0	5 (9.61%)	1 (2.17%)
No. of embryos with extracardiac malformations[b]	0	6 (11.53%)	2 (4.34%)

[a] Cardiac malformation such as persistent truncus arteriosus with ventricular septal defects and defective endocardial cushion.
[b] Extracardiac malformation such as neural tube defects, including exencephaly, anencephaly, and spina bifida.

Malondialdehyde concentration

Cardiac lipid peroxidation in embryos of study groups was determined by thiobarbituric acid-reactive substance (TBARS) assay. The amount of malondialdehyde (MDA) was significantly increased ($P<0.001$) in the developing heart of embryos from diabetic mice when compared to controls (Fig. 2C). However, the MDA concentration markedly declined after Zn supplementation.

Cytosolic and mitochondrial superoxide dismutase activity

The embryos in each of the study groups were analyzed for cytosolic (Fig. 3A) and mitochondrial (Fig. 3B) superoxide dismutase (SOD) activity at two different time points. As shown in Fig. 3, significant decrease was observed in both cytosolic and mitochondrial SOD activity of embryos from the diabetic group when compared to both control and Zn-supplemented diabetic groups at both time points (E13.5 and E15.5). This shows that embryos from the diabetic group were the variable associated with reduced embryonic SOD activity.

Oxidized and reduced glutathione levels

Oxidized and reduced glutathione activity in the developing heart at E13.5 and E15.5 was performed. The result showed that a significant alteration in GSSG (Fig. 4A) and GSH (Fig. 4B) levels was observed in the developing heart of embryos from diabetic mice when compared to controls. Therefore, the present result

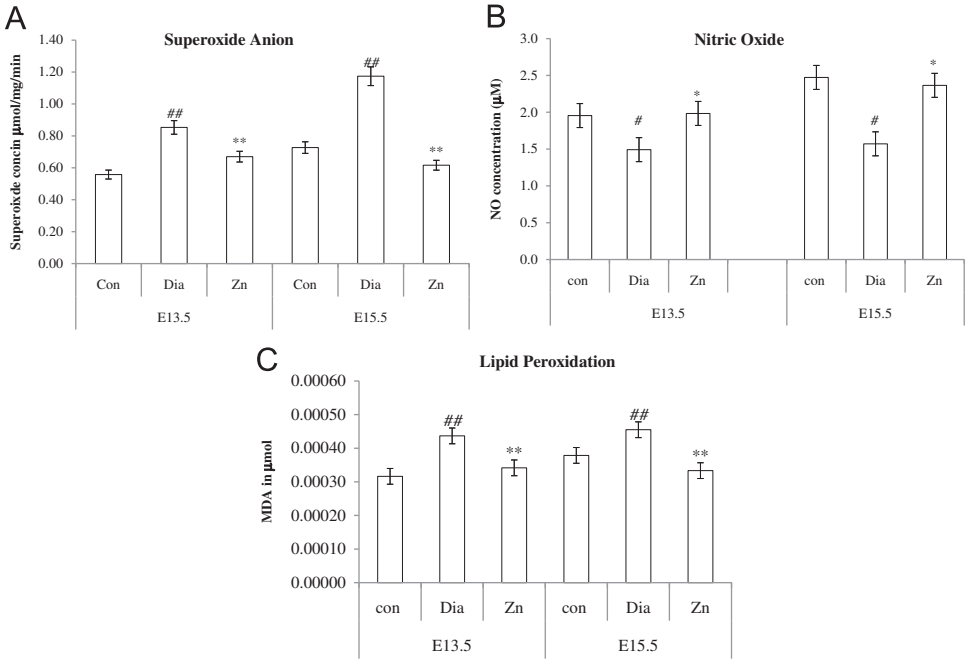

Fig. 2. (A) Determination of superoxide anion by colorimetric assay in the developing heart at E13.5 and E15.5. The cardiac superoxide anion is significantly decreased in the developing heart of embryos from Zn-supplemented diabetic mice when compared to diabetic mice. Data represent the mean ± SD. $^{\#\#}P<0.001$ control vs diabetic, $^{**}P<0.001$ diabetic vs Zn-supplemented diabetic. (B) Determination of nitric oxide (NO) by colorimetric assay in the developing heart at E13.5 and E15.5. The total amount of NO is significantly increased in the developing heart of embryos from Zn-supplemented diabetic mice when compared to diabetic mice. Data represent the mean ± SD. $^{\#}P<0.05$ control vs diabetic, $^{*}P<0.05$ diabetic vs Zn-supplemented diabetic. (C) Determination of lipid peroxidation by TBARS assay in the developing heart at E13.5 and E15.5. The amount of malondialdehyde (MDA) is significantly decreased in the developing heart of embryos from Zn-supplemented diabetic mice when compared to diabetic mice. Data represent the mean ± SD. $^{\#\#}P<0.001$ control vs diabetic, $^{**}P<0.001$ diabetic vs Zn-supplemented diabetic.

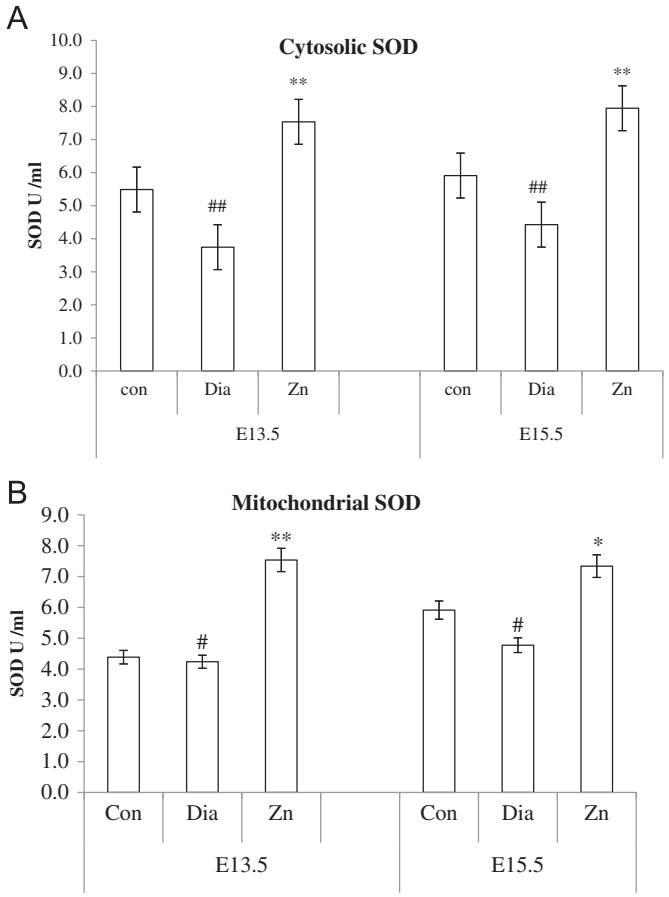

Fig. 3. (A) Determination of cytosolic superoxide dismutase (SOD) by colorimetric assay in the developing heart at E13.5 and E15.5. The cytosolic SOD is significantly increased in the developing heart of embryos from Zn-supplemented diabetic mice when compared to diabetic mice. Data represent the mean ± SD. $^{\#\#}P < 0.001$ control vs diabetic, $^{**}P < 0.001$ diabetic vs Zn-supplemented diabetic. (B) Determination of mitochondrial SOD by colorimetric assay in the developing heart at E13.5 and E15.5. The mitochondrial SOD is significantly increased in the developing heart of embryos from the Zn-supplemented diabetic group when compared to other groups. Data represent the mean ± SD. $^{\#}P < 0.05$, $^{\#\#}P < 0.001$ control vs diabetic, $^{*}P < 0.05$, $^{**}P < 0.001$ diabetic vs Zn-supplemented diabetic.

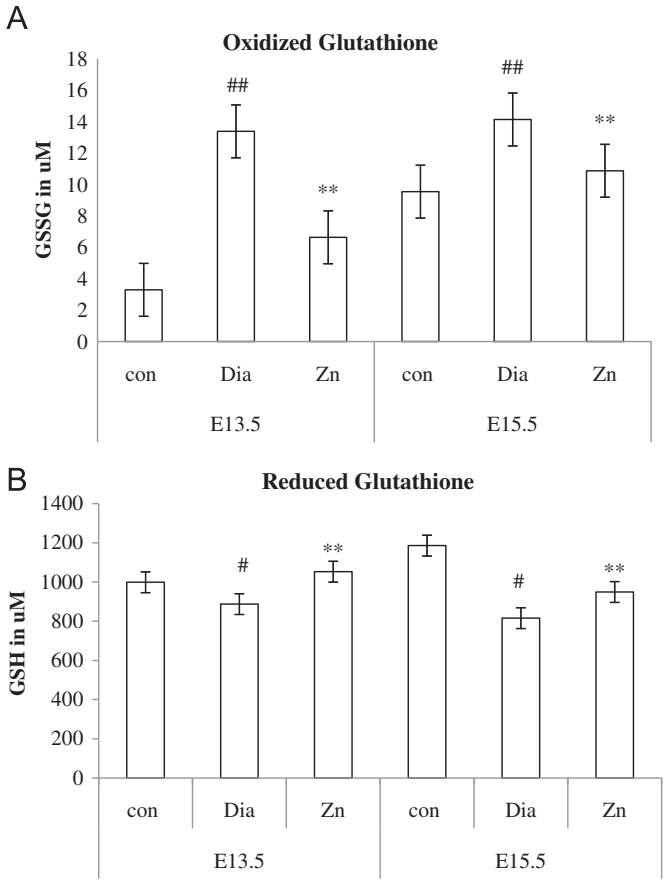

Fig. 4. (A) Determination of oxidized glutathione (GSSG) by colorimetric assay in the developing heart at E13.5 and E15.5. The level of GSSG is significantly decreased in the developing heart of embryos from Zn-supplemented diabetic mice when compared to diabetic mice. Data represent the mean ± SD. $^{\#\#}P < 0.001$ control vs diabetic, $^{**}P < 0.001$ diabetic vs Zn-supplemented diabetic. (B) Determination of reduced glutathione (GSH) by colorimetric assay in the developing heart at E13.5 and E15.5. The level of GSH is significantly increased in the developing heart of embryos from Zn-supplemented diabetic mice when compared to diabetic mice. Data represent the mean ± SD. $^{\#}P < 0.05$ control versus diabetic, $^{**}P < 0.001$ diabetic vs Zn-supplemented diabetic.

suggests the existence of oxidative stress in the developing heart of embryos from diabetic mice. However, the levels of GSSG and GSH levels were significantly altered in the developing heart of embryos from Zn-supplemented diabetic group when compared to other groups.

mRNA expression of MT-1

Real-time RT-PCR analysis revealed a significant decrease ($P < 0.001$) in the mRNA expression of metallothionein-1 (MT-1) in the developing heart of embryos from diabetic mice when compared to controls (Fig. 5A). However, the mRNA expression of MT-1 was rescued by Zn supplementation.

Immunohistochemistry analysis

In embryos of control mice, MT immunoreactivity was expressed in cardiomyocytes in the ventricular myocardium (Fig. 5B). In contrast, MT protein expression was reduced in cardiomyocytes in the EC, in the ventricular myocardium in the embryos from diabetic mice (Fig. 5C). However, the MT protein expression was rescued by Zn supplementation (Fig. 5D).

Nuclear microscopy analysis

Nuclear microscopy, a suite of imaging techniques which compose RBS and STIM, was used to simultaneously map and quantify the elemental information present in the samples. The developing heart including EC, and the OFT of all the groups were sectioned and stained by H&E (Figs. 6A, G, and M). The lesion area was identified on the basis of structural landmarks (trace element deposits) in the images of STIM. The developing heart sections from control (Figs. 6B–F), diabetic (Figs. 6H–L), and Zn-supplemented diabetic (Figs. 6N–R) mice embryos showed distinct levels of trace element contents (P, Ca, Fe, and Zn) in the nuclear microscopy images. A novel PIXE technique was used for quantification of the trace elements. The trace elements (P: 9889 ± 1074 ppm, Ca: 453 ± 121 ppm, and Zn: 83 ± 13 ppm) in the EC were significantly increased ($P < 0.001$) in the embryos from the Zn-supplemented diabetic group when compared to that of the diabetic group (P, 7429 ± 1383 ppm; Ca, 490 ± 129 ppm; and Zn, 68 ± 19 ppm) (Figs. 7A, B, and D). However, the Fe level in the EC was significantly decreased ($P < 0.05$) in the Zn-supplemented diabetic (105 ± 15 ppm) group as compared with those of diabetic and control (473 ± 110 ppm) groups (Fig. 7C). A similar decrease of Fe level was also detected in the OFT region, which lies adjacent to the EC area in the embryos from the Zn-supplemented diabetic (70 ± 6 ppm) group when compared to the

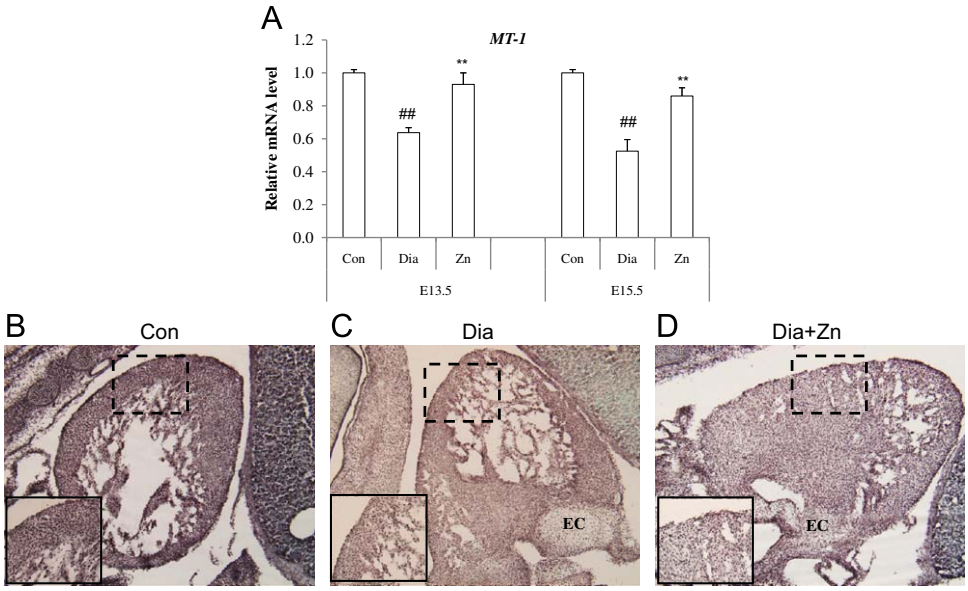

Fig. 5. (A) Real-time RT-PCR analysis of MT-1 mRNA expression in the developing heart at E13.5 and E15.5. Bar graph representing the fold changes of mRNA levels quantified by normalization to the β-actin as an internal control. $^{\#\#}P < 0.001$ control vs diabetic, $^{**}P < 0.001$ diabetic vs Zn-supplemented diabetic. (B–D) Sagittal sections of the thoracic region of the whole embryos (E.13.5) of control (B), diabetic (C), and Zn-supplemented diabetic (D) mice show the immunoreactivity of MT. The MT immunoreactivity appears to be down-regulated in cardiomyocytes in the EC, in the ventricular myocardium in the embryos of diabetic (C) as compared with those of Zn-supplemented diabetic (D) and control (B) mice. Magnification $\times 100$. Inset shows high magnification of the cardiomyocytes expressing MT immunoreactivity in the ventricular myocardium (B–D). Magnification $\times 200$.

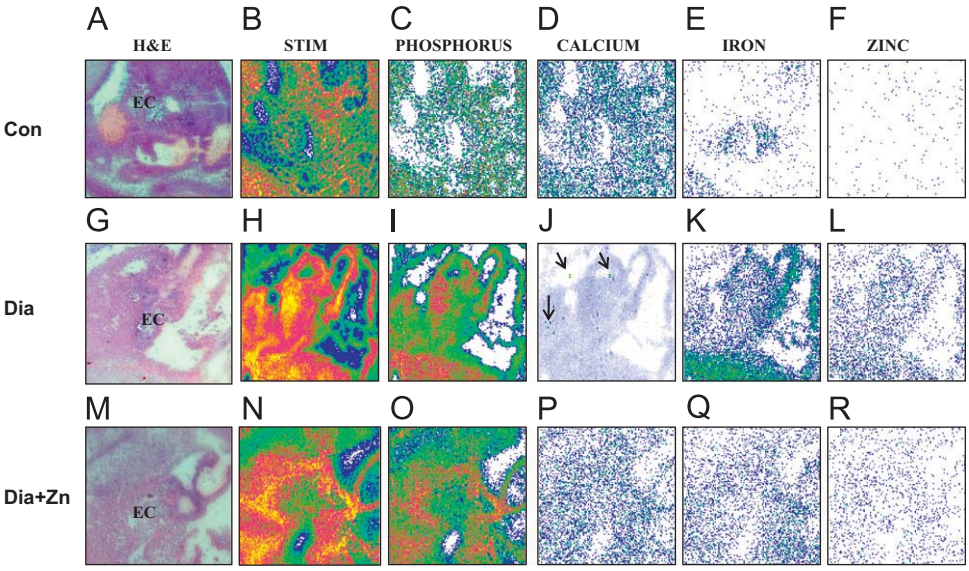

Fig. 6. STIM maps show the trace element contents (P, Ca, Fe, and Zn) in the endocardial cushion (EC) of embryos from control (B), diabetic (H), and Zn-supplemented diabetic (N) mice. A PIXE technique shows that trace elements such as P (I) and Ca (J) appear to be decreased whereas the Fe (K) level appears to be increased in the developing heart of embryos from diabetic mice when compared to Zn-supplemented diabetic mice. Embryos from Zn-supplemented diabetic mice show normal architecture and trace element Fe content (Q) appears to be decreased in the developing heart.

diabetic group (108 ± 8 ppm). In this study, we showed that the Zn may reduce diabetic complications by decreasing iron levels in the lesion, possibly leading to the inhibition of iron-catalyzed free radical reactions.

In vitro studies

The ROS assay revealed that the high glucose concentration impaired cell viability and enhanced apoptosis in cardiomyocytes via excessive generation of ROS, forming one of the bases for cardiac malformations as seen in cells from diabetic conditions. Further, augmented ROS activation was observed in H9c2 cells following the glucose exposure at 5.5 and 44 mM concentrations (Fig. 8). Whereas, Zn supplementation inhibited oxidative stress-induced H9c2 damage and inhibition of ROS generation and the augmentation of Zn activation may be involved in the protective effect (Fig. 8).

Cell cycle analysis

Cell cycle analysis showed that about 60.4 and 70% of myoblast cells were in sub-G1 phase at 5.5 mM (Fig. 9A) and 44 mM (Fig. 9B) glucose concentrations, respectively. In contrast, cells treated with 44 mM Zn showed that about 7.15% of cells were in sub-G1 phase (Fig. 9D) which was almost similar to the control cells and the 5.5 mM Zn-treated cells (Fig. 9C).

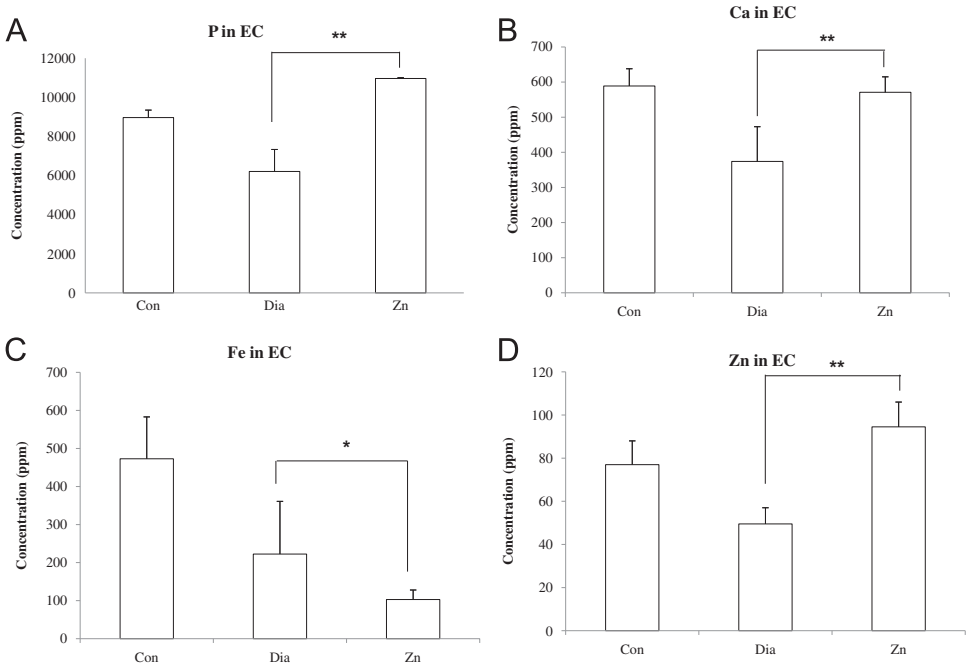

Fig. 7. Quantitative analysis shows that phosphorus (A), calcium (B), and zinc (D) levels are significantly increased whereas the iron (C) level is significantly decreased in the EC of embryos from Zn-supplemented diabetic mice when compared to diabetic mice. Mean values ± SD. $^{*}P < 0.05$, $^{**}P < 0.001$ diabetic vs Zn-supplemented diabetic.

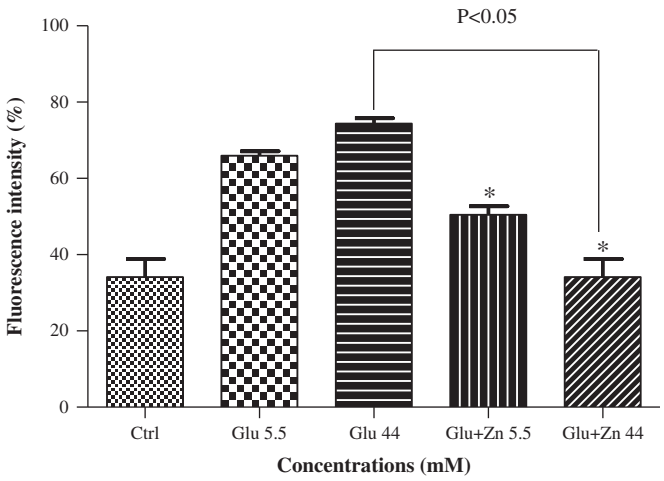

Fig. 8. Flow cytometry analysis shows the percentage of reactive oxygen species (ROS) in H9c2 cells treated with different concentrations (5.5 and 44 mM) of glucose alone or in combination of Zn at 24 h. The ROS is significantly decreased in cells treated with both 5.5 and 44 mM concentrations of glucose supplemented with Zn at 24 h. $^{*}P < 0.05$.

TUNEL staining

In addition, the results obtained from TUNEL staining also confirmed that apoptosis was taking place. The H9c2 cells treated with high glucose concentrations induced cell death and apoptosis due to the oxidative stress (Figs. 10A and B) compared to the Zn-treated cells (Figs. 10C and D). The cell morphology was completely changed and DNA breaking was evident (Figs. 10A and B). However, the Zn-treated cells appeared to be protected at 5.5 and 44 mM glucose concentration from apoptosis (Figs. 10C and D).

Discussion

The maternal blood glucose level of diabetic and Zn-supplement diabetic groups was higher (> 16 mmol/L) than that of the control group (4–6 mmol/L). The developmental stage E13.5 was chosen for this study, as it corresponds to ~6 weeks of human gestation [25,26], when all 4 chambers of the heart were clearly distinguishable, and the outflow tract was evident [18]. In addition, the heart phenotype was apparent in embryos from diabetic mice [3,4]. Embryos with malformations from diabetic group, normal embryos from Zn-supplemented diabetic; and nondiabetic control were used in this study. Recently, we reported that there is an association between maternal diabetes and dysmorphogenesis in mouse embryos derived from diabetic pregnancy [3,4]. The reduction in number of embryos observed in diabetic pregnancies could be due to either reduced fecundity or early embryonic lethality resulting from a higher malformation rate in the embryos of diabetic mothers compared with those of nondiabetic mothers [27]. The morphological phenotypes observed in maternal diabetes in the present study appear similar to the features of cardiac and extracardiac malformations seen in the offspring of diabetic mothers [27–29]. The increased number of embryos from Zn-supplemented diabetic group may possibly explain that Zn supplement reduces early embryonic lethality resulting from a higher mortality rate in the embryos of diabetic mothers compared with those of Zn-supplemented-diabetic mothers. Altered expression of several genes involved in the development of cardiac neural crest (including Bmp4, Msx1, and Pax3) appears to contribute to the pathogenesis of maternal diabetes-induced congenital heart defects in mice [3]. Further, hyperglycemia altered the expression of endothelial nitric oxide synthase (eNOS) and vascular endothelial growth factor (VEGF) genes that are involved in the regulation of cell growth and vasculogenesis, thereby contributing to the cardiac malformations in embryos from diabetic mice [4]. A catalase and GPx activity were reported to be unchanged in hyperglycemia-induced malformation with slightly increased activity of SOD [65]. On the other hand, decreased levels of SOD and GPx were observed in diabetic animals [30]. In the present study, the cytosolic and mitochondrial SOD was found to be decreased in the developing heart of embryos from diabetic mice. Hypoinsulinemia initiates β-oxidation of fatty acids by activating fatty acyl

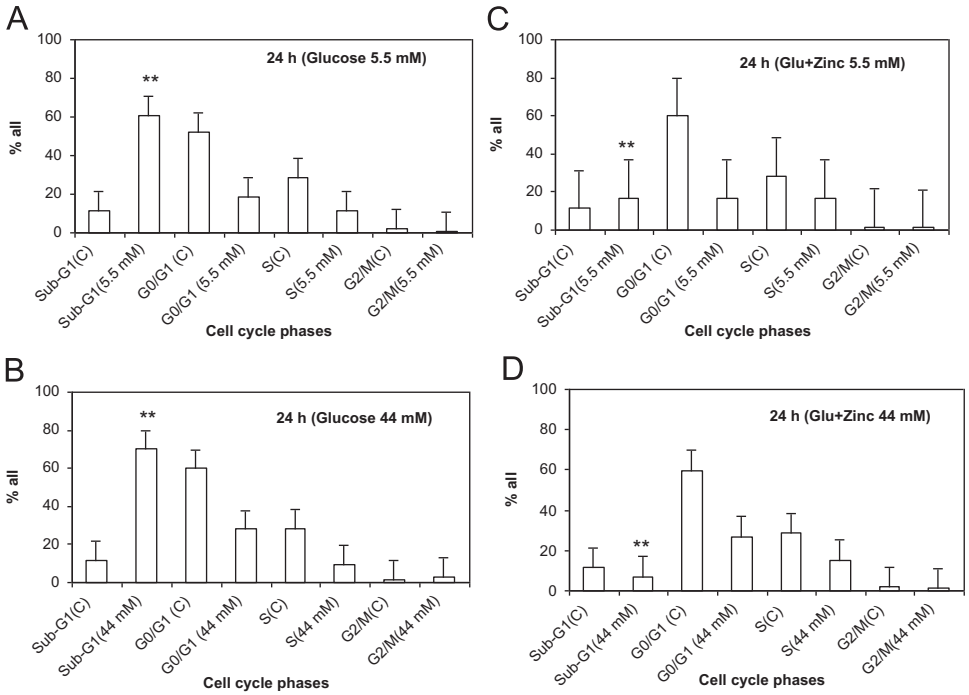

Fig. 9. Cell cycle analysis shows the different phases of the cell cycle treated with 5.5 mM glucose (A), 44 mM glucose (B), 5.5 mM glucose + Zn (C), 44 mM glucose + Zn (D) concentrations at 24 h. The sub-G1 phase (apoptotic phase) is significantly increased in cells treated with 5.5 and 44 mM glucose concentrations at 24 h. In contrast, the sub-G1 phase is markedly decreased in cells treated with 5.5 and 44 mM concentrations of glucose supplemented with Zn at 24 h. $^{**}P < 0.001$.

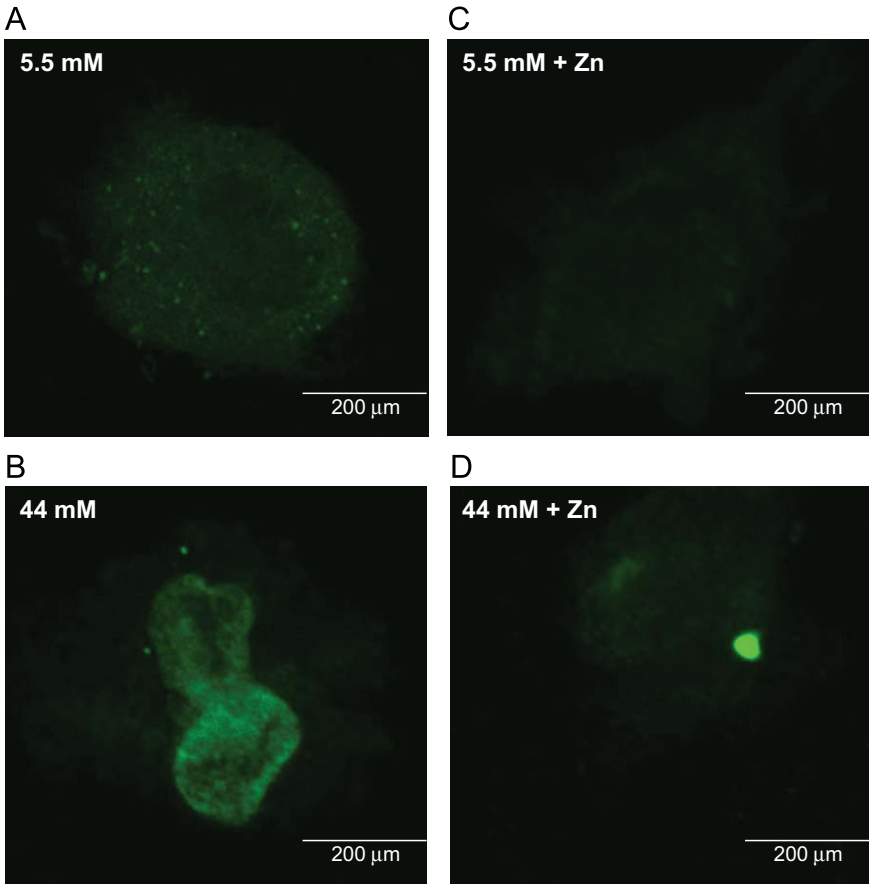

Fig. 10. The TUNEL staining (which stains nuclei with fragmented DNA) shows the H9c2 cells treated with 5.5 mM glucose (A), 44 mM glucose (B), 5.5 mM glucose + Zn (C), 44 mM glucose + Zn (D) concentrations at 24 h. H9c2 cells treated with 5.5 and 44 mM glucose concentrations show morphological changes and nucleus disintegration (A, B). Zn-treated cells did not show any morphological changes or cell death (C, D).

CoA oxidase, which results in the production of hydrogen peroxide, and inactivates the SOD. Reduced activity of SOD may be due to its depletion and inhibition by increased free radicals [31]. Zn is also a transition metal which may protect the oxidation of sulfhydryl groups and inhibit production of reactive oxygen species [32]. Some trace elements (such as Zn, Cu, and Se) are commonly referred to as antioxidant nutrients, but they do not themselves possess any antioxidant properties, instead they are required for the activity of some antioxidant enzymes [33]. Recent studies have shown that the levels of Zn [34,35] and Se [34,36] are lower in women with gestational diabetes mellitus (GDM). The activity CuZnSOD is sensitive to tissue Cu as these enzymes require Cu as a catalytic cofactor. The increase in CuZnSOD activity observed in GDM may be due to Zn and Cu levels in GDM. Consistent with this hypothesis, compared with normal pregnant women, the Cu contents in serum of pregnant women with GDM are increased [35]. This is also consistent with the ability of Cu to produce excessive amounts of ROS. Results from the present study appear to suggest that increased activity of SOD in the developing heart of embryos from Zn-supplemented diabetic mice may possibly explain that Zn reduces the oxidative stress mediated by SOD in embryos of diabetic mice as Zn is a cofactor for SOD. However, SOD activity in the present study has certain limitations that need to be taken into account: (a) purity of mitochondrial preparations and analyses of Cu/Zn protein need to be tested; (b) changes in SOD activity were relatively small (2 U/ml) which lead to questions about biological effects. Thus, further studies on genomic expression level of antioxidant enzymes in oxidative damage caused by ROS are required.

Lipid peroxidation is significantly increased in the developing heart of embryos from diabetic mice. Major end products of lipid peroxidation, such as hydroperoxides, alter the biosynthesis of prostaglandin by inhibiting the production of prostacyclin and enhance the production of thromboxane A2 [37]. This imbalance may lead to deleterious effects on embryos, thereby resulting in development of diabetes-related embryopathy. Several markers of lipid peroxidation are available with different degrees of specificity, from MDA as a global marker to F2-isoprostane, which is specifically produced from arachidonic acid. Among these, MDA has been widely studied as a product of lipid peroxidation by the thiobarbituric assay [38]. Further, MDA and thiobarbituric acid reactivity were used as diagnostic indices of lipid peroxidation and peroxidative tissue injury [39]. Measurements of lipid peroxidation include MDA, 4-hydroxynonenal, TBARS, and LOOH. Maternal MDA levels in serum and plasma are increased in GDM women compared to normal glucose tolerant (NGT) pregnant women [40–42]. Also, enhanced levels of TBARS [43,44] have been reported in diabetic women. Further, there is a significant positive correlation between maternal HbA1c and MDA [41,45,46], suggesting that higher levels of lipid peroxidation are evident in patients with poor glycemic control [33]. The MDA concentration was significantly decreased in the Zn-supplemented diabetic group. It seems that Zn directly acts a major antioxidant defense against diabetes-induced oxidative damage or indirectly it binds and stabilizes the membrane and prevents the membrane lipid oxidative damage, thereby suppressing the lipid peroxidation [47,48]. The presence of Zn prevents lipid peroxidation and thus Zn may play a role in protecting the cell from oxidative stress [49]. However, further work is warranted to explore the specificity of MDA as F2-isoprostanes are considered to be some of the best lipid peroxidation markers [50].

Glutathione is one of the primary antioxidant defenses during oxidative stress. In diabetic conditions, mitochondrial oxidative stress such as GSH depletion leads to cardiac cell death [51]. GSH depletion and impaired responsiveness of GSH-synthesizing enzyme to oxidative stress during organogenesis may have important roles in the development of embryonic malformations in diabetes [52]. In the present study, GSH level was significantly decreased and GSSG level was significantly increased in the developing heart of embryos from diabetic mice. However, Zn supplementation reversed these changes. Zn supplementation to diabetic mice has been shown to reduce oxidative stress via induction of cardiac MT which is the primary antioxidant activity against ROS and RNS [53].

Nitric oxide (NO) has been proposed to act as a prooxidant at high concentrations or when it reacts with superoxide radicals ($\cdot O_2^-$), forming the highly reactive peroxynitrite ($ONOO^-$). Conversely, $NO\cdot$ can inhibit oxidation and terminate chain reactions during lipid peroxidation [54]. In the present study, NO concentrations were found to be decreased in the developing heart of embryos from diabetic mice but this condition is reverted back in the Zn-supplemented diabetic group. Further, superoxide anions were significantly increased in the diabetes group whereas they were decreased in the Zn-supplemented diabetic group. This alteration may be due the antioxidant activity of Zn alone, Zn induction of MT, or Zn inhibition of redox-sensitive transcription factors [55]. Formations of superoxide and 3-nitrotyrosine (3-NT), a marker for peroxynitrite-induced protein damage, were found in the heart of wild-type diabetic mice [56]. Increases in 3-NT formation and cytotoxicity were observed in wild-type, but not in metallothionein-overexpressing transgenic (MT-TG), cardiomyocytes. Either urate, a peroxynitrite-specific scavenger, or Mn (111) tetrakis 1-methyl 4-pyridyl porphyrin pentachloride (MnTMPyP), a SOD mimic, inhibited the formation of 3-NT along with a significant prevention of cytotoxicity [56]. It has been suggested that MT prevention of diabetic cardiomyopathy is mediated, at least in part, by suppression of superoxide generation and associated nitrosative damage.

MT prevents diabetic cardiomyopathy and suppresses oxidative damage in the STZ-induced diabetic mouse model. MT is a cysteine-rich protein, it acts as an antioxidant, and it is very efficient in scavenging or quenching various free radicals or ROS. Zn ions might also induce the synthesis of MT, which suppresses the free radicals produced by hyperglycemia [7,56]. Zn concentration ensures the specificity of Zn transfer, thereby allowing for the appropriate regulation of the function of the Zn-binding proteins in response to changes in the intracellular environment [7,10,57]. Such direct transfer of Zn from MT may lead to modification of signaling pathways of specific proteins under oxidative stress, thereby resulting in cardioprotection against oxidative damage [58]. In the present study, the MT gene expressions were significantly down-regulated in the developing heart at E13.5 and E15.5 from the diabetic group, but it was reversed in the Zn-supplemented diabetic group. We have demonstrated that MT-1 protein expression is increased in the developing heart of embryos from the Zn-supplemented diabetic group when compared with the diabetic group. In response to the diabetes-induced oxidative stress, cardiac antioxidant defense mechanisms are activated to protect the embryonic heart from the deleterious effects of hyperglycemia, by MT, which may take place because MT is markedly restored after Zn supplementation.

Nuclear microscopy (MeV ion-based) techniques have the ability to image density variations in relatively thick tissues, map trace elements at the cellular level, and extract quantitative information on these elements [59]. In the present study, the trace elements such as P, Ca, and Zn were deposited more in the EC and the OFT in embryos obtained from the Zn-supplemented diabetic group. Interestingly, the Fe content was reduced in the Zn-supplemented group when compared to the diabetic group. It is generally believed that some trace elements (Zn, Cu, Mn, and Se) play a major role in protecting the insulin-secreting pancreatic

beta cells, which are sensitive to free radical damage [14,15]. Another study has indicated that diabetic individuals are vulnerable to trace element deficiency [60]. Several studies have also documented this phenomenon by using supplements of potential "antidiabetic minerals" such as Zn, Cu, Mn, and Se and have yielded some promising positive results [61]. Maternal and fetal Zn, Cu, Mn, Fe, Mg, and Ca levels have been studied in diabetic rats [62–64]. Maternal Cu and Zn levels were higher in the liver and kidneys of diabetic rats. In contrast, the Zn level was significantly decreased in the fetus of a diabetic pregnancy. It has been suggested that diabetes may induce fetal Zn deficiency and could be one of the mechanisms of the teratogenicity of the diabetic state. In the present study, there was significant reduction of Zn levels in the developing heart of embryos from diabetic mice compared to normal controls. Conversely, the fetal Zn level was greatly increased in the heart of Zn-supplemented diabetic mice when compared to controls. Besides, Zn may have an antidiabetic effect by decreasing iron levels in the lesion sites, possibly leading to the inhibition of iron-catalyzed free radical reactions.

The alteration in the ROS has been shown to be associated with fetal malformations in diabetic pregnancy [65,66]. Increased ROS formation, which in turn promotes cardiomyocytes apoptosis, is associated with the pathogenesis and progression of cardiac diseases [67,68]. Our results corroborate those of a previous report that cell cycle progression and survival of cardiomyocytes were impaired by high concentrations of glucose [69]. The H9c2 cells exposed to high glucose supplemented with Zn significantly suppress the intercellular ROS formation and stress-induced oxidative death at 24 h. It has been reported the ROS-induced cell death may be the result of the activation of AMPK in H9c2 cells [70].

The cell cycle analysis revealed that 70% of myoblast cells were in sub-G1 phase (apoptotic phase) at high glucose concentrations at 24 h. However, the myoblast cells treated with high glucose supplemented with Zn showed that about 7.15% of the cells were in sub-G1 phase at 24 h, which was almost similar to the control cells. Our results are in agreement with Song et al. [7] who earlier reported that Zn supplementation helps to prevent or delay diabetic cardiomyopathy.

TUNEL staining also supported the cell cycle results that high glucose induced cell death (apoptosis) and morphological changes at 24 h. However, the Zn-supplemented H9c2 cells were protected from glucose-induced apoptosis. Similar results were reported by Kumar and Sitasawad [71]. In particular, it is well known that Zn can inhibit the activation of caspase 3 and thereby prevent caspase 3-dependent apoptosis [72] and that Zn inhibits the doxorubicin-activated calcineurin signal transduction pathway in H9c2 cells [57].

The present study reveals that oxidative stress in embryonic cardiac tissues responds differently to the adverse environment created by maternal diabetes during pregnancy. It also suggests that Zn has both antioxidative and antiapoptotic activities against glucose-induced oxidative stress through the inhibition of mitochondrial damage in embryonic cardiomyocytes. The adverse effects of maternal diabetes on an unborn fetus could possibly be treated by Zn supplementation in the early stages of gestational diabetic pregnancy.

Acknowledgments

This work was supported by research grants from the BMRC (R-181-000-081-305) and Academic Research Fund (R-181-000-075-112), National University of Singapore, Singapore.

References

[1] Eriksson, U. J.; Borg, L. A.; Cederberg, J.; Nordstrand, H.; Siman, C. M.; Wentzel, C.; Wentzel, P. Pathogenesis of diabetes-induced congenital malformations. *Ups. J. Med. Sci.* **105:**53–84; 2000.
[2] Reece, E. A.; Eriksson, U. J. The pathogenesis of diabetes-associated congenital malformations. *Obstet. Gynecol. Clin. North Am.* **23:**29–45; 1996.
[3] Kumar, S. D.; Dheen, S. T.; Tay, S. S. Maternal diabetes induces congenital heart defects in mice by altering the expression of genes involved in cardiovascular development. *Cardiovasc. Diabetol.* **6:**34; 2007.
[4] Kumar, S. D.; Yong, S. K.; Dheen, S. T.; Bay, B. H.; Tay, S. S. Cardiac malformations are associated with altered expression of vascular endothelial growth factor and endothelial nitric oxide synthase genes in embryos of diabetic mice. *Exp. Biol. Med. (Maywood)* **233:**1421–1432; 2008.
[5] Son, S. M. Role of vascular reactive oxygen species in development of vascular abnormalities in diabetes. *Diabetes Res. Clin. Pract* **77(Suppl. 1):**S65–S70; 2007.
[6] Rahimi, R.; Nikfar, S.; Larijani, B.; Abdollahi, M. A review on the role of antioxidants in the management of diabetes and its complications. *Biomed. Pharmacother.* **59:**365–373; 2005.
[7] Song, Y.; Wang, J.; Li, X. K.; Cai, L. Zinc and the diabetic heart. *Biometals* **18:**325–332; 2005.
[8] Schwarz, M. A.; Lazo, J. S.; Yalowich, J. C.; Allen, W. P.; Whitmore, M.; Bergonia, H. A.; Tzeng, E.; Billiar, T. R.; Robbins, P. D.; Lancaster Jr J. R., et al. Metallothionein protects against the cytotoxic and DNA-damaging effects of nitric oxide. *Proc. Natl. Acad. Sci. USA* **92:**4452–4456; 1995.
[9] Zhou, Z.; Sun, X.; Lambert, J. C.; Saari, J. T.; Kang, Y. J. Metallothionein-independent zinc protection from alcoholic liver injury. *Am. J. Pathol.* **160:**2267–2274; 2002.
[10] Kang, Y. J. Metallothionein redox cycle and function. *Exp. Biol. Med. (Maywood)* **231:**1459–1467; 2006.
[11] Ohly, P.; Dohle, C.; Abel, J.; Seissler, J.; Gleichmann, H. Zinc sulphate induces metallothionein in pancreatic islets of mice and protects against diabetes induced by multiple low doses of streptozotocin. *Diabetologia* **43:**1020–1030; 2000.
[12] Masaki, H.; Ochiai, Y.; Okano, Y.; Yagami, A.; Akamatsu, H.; Matsunaga, K.; Sakurai, H.; Suzuki, K. A zinc(II)-glycine complex is an effective inducer of metallothionein and removes oxidative stress. *J. Dermatol. Sci.* **45:**73–75; 2007.
[13] Watt, F.; Van Kan, J. A.; Rajta, I.; Bettiol, A. A.; Choo, T. F.; Breese, M. B. H.; Osipowicz, T. The National University of Singapore high energy ion nanoprobe facility: performance tests. *Nucl. Instrum. Methods Phys. Res.* ***B*** **210:**14–20; 2003.
[14] Williams, N. R.; Rajput-Williams, J.; West, J. A.; Nigdikar, S. V.; Foote, J. W.; Howard, A. N. Plasma, granulocyte and mononuclear cell copper and zinc in patients with diabetes mellitus. *Analyst* **120:**887–890; 1995.
[15] Al-Awadi, F. M.; Anim, J. T.; Srikumar, T. S.; Al-Rustom, M. Possible role of trace elements in the hypoglycemic effect of plants extract in diabetic rats. *J. Trace Elements Exp. Med* **17:**31–44; 2004.
[16] Sissman, N. J. Developmental landmarks in cardiac morphogenesis: comparative chronology. *Am. J. Cardiol.* **25:**141–148; 1970.
[17] Kaufman, K. H. *The atlas of mouse development*. New York, NY: Academic Press; 1992.
[18] Srinivasan, S.; Baldwin, H. S.; Aristizabal, O.; Kwee, L.; Labow, M.; Artman, M.; Turnbull, D. H. Noninvasive, in utero imaging of mouse embryonic heart development with 40-MHz echocardiography. *Circulation* **98:**912–918; 1998.
[19] Ohkawa, H.; Ohishi, N.; Yagi, K. Assay for lipid peroxides in animal tissues by thiobarbituric acid reaction. *Anal. Biochem.* **95:**351–358; 1979.
[20] Ingelman-Sundberg, M.; Johansson, I. Mechanisms of hydroxyl radical formation and ethanol oxidation by ethanol-inducible and other forms of rabbit liver microsomal cytochromes P-450. *J. Biol. Chem* **259:**6447–6458; 1984.
[21] Livak, K. J.; Schmittgen, T. D. Analysis of relative gene expression data using real-time quantitative PCR and the 2(-delta delta C(T)) method. *Methods* **25:**402–408; 2001.
[22] De Vriese, A. S.; Verbeuren, T. J.; Van de Voorde, J.; Lameire, N. H.; Vanhoutte, P. M. Endothelial dysfunction in diabetes. *Br. J. Pharmacol.* **130:**963–974; 2000.
[23] Minqin, R.; Watt, F.; Huat, B. T.; Halliwell, B. Correlation of iron and zinc levels with lesion depth in newly formed atherosclerotic lesions. *Free Radic. Biol. Med.* **34:**746–752; 2003.
[24] Yosef, H.; Tamhane, A. C. *Multiple comparison procedures*. New York: Wiley; 1987.
[25] Sissman, N. J. Developmental landmarks in cardiac morphogenesis: comparative chronology. *Am. J. Cardiol.* **25:**141–148; 1970.
[26] Kaufman, M. *The atlas of mouse development*. New York, NY: Academic Press; 1992.
[27] Phelan, S. A.; Ito, M.; Loeken, M. R. Neural tube defects in embryos of diabetic mice: role of the Pax-3 gene and apoptosis. *Diabetes* **46:**1189–1197; 1997.
[28] Molin, D. G.; Roest, P. A.; Nordstrand, H.; Wisse, L. J.; Poelmann, R. E.; Eriksson, U. J.; Gittenberger-De Groot, A. C. Disturbed morphogenesis of cardiac outflow tract and increased rate of aortic arch anomalies in the offspring of diabetic rats. *Birth Defects Res. A Clin. Mol. Teratol* **70:**927–938; 2004.
[29] Ferencz, C.; Rubin, J. D.; McCarter, R. J.; Clark, E. B. Maternal diabetes and cardiovascular malformations: predominance of double outlet right ventricle and truncus arteriosus. *Teratology* **41:**319–326; 1990.

[30] Sivan, E.; Lee, Y. C.; Wu, Y. K.; Reece, E. A. Free radical scavenging enzymes in fetal dysmorphogenesis among offspring of diabetic rats. *Teratology* **56:**343–349; 1997.
[31] Damasceno, D. C.; Volpato, G. T.; de Mattos Paranhos Calderon, I.; Cunha Rudge, M. V. Oxidative stress and diabetes in pregnant rats. *Anim. Reprod. Sci.* **72:**235–244; 2002.
[32] Ertekin, M. V.; Karslioglu, I.; Erdem, F.; Sezen, O.; Gepdiremen, A.; Serifoglu, K. Zinc sulfate in the prevention of total-body irradiation-induced early hematopoietic toxicity: a controlled study in a rat model. *Biol. Trace Elem. Res.* **100:**63–73; 2004.
[33] Lappas, M.; Hiden, U.; Desoye, G.; Froehlich, J.; Hauguel-de Mouzon, S.; Jawerbaum, A. The role of oxidative stress in the pathophysiology of gestational diabetes mellitus. *Antioxid. Redox Signal.* **15:**3061–3100; 2011.
[34] Bo, S.; Lezo, A.; Menato, G.; Gallo, M. L.; Bardelli, C.; Signorile, A.; Berutti, C.; Massobrio, M.; Pagano, G. F. Gestational hyperglycemia, zinc, selenium, and antioxidant vitamins. *Nutrition* **21:**186–191; 2005.
[35] Wang, Y.; Tan, M.; Huang, Z.; Sheng, L.; Ge, Y.; Zhang, H.; Jiang, M.; Zhang, G. Elemental contents in serum of pregnant women with gestational diabetes mellitus. *Biol. Trace Elem. Res.* **88:**113–118; 2002.
[36] Kilinc, M.; Guven, M. A.; Ezer, M.; Ertas, I. E.; Coskun, A. Evaluation of serum selenium levels in Turkish women with gestational diabetes mellitus, glucose intolerants, and normal controls. *Biol. Trace Elem. Res.* **123:**35–40; 2008.
[37] Tesfamariam, B. Free radicals in diabetic endothelial cell dysfunction. *Free Radic. Biol. Med.* **16:**383–391; 1994.
[38] Gavino, V. C.; Miller, J. S.; Ikharebha, S. O.; Milo, G. E.; Cornwell, D. G. Effect of polyunsaturated fatty acids and antioxidants on lipid peroxidation in tissue cultures. *J. Lipid Res.* **22:**763–769; 1981.
[39] Janero, D. R. Malondialdehyde and thiobarbituric acid-reactivity as diagnostic indices of lipid peroxidation and peroxidative tissue injury. *Free Radic. Biol. Med* **9:**515–540; 1990.
[40] Kharb, S. Lipid peroxidation in pregnancy with preeclampsia and diabetes. *Gynecol. Obstet. Invest.* **50:**113–116; 2000.
[41] Peuchant, E.; Brun, J. L.; Rigalleau, V.; Dubourg, L.; Thomas, M. J.; Daniel, J. Y.; Leng, J. J.; Gin, H. Oxidative and antioxidative status in pregnant women with either gestational or type 1 diabetes. *Clin. Biochem.* **37:**293–298; 2004.
[42] Madazli, R.; Tuten, A.; Calay, Z.; Uzun, H.; Uludag, S.; Ocak, V. The incidence of placental abnormalities, maternal and cord plasma malondialdehyde and vascular endothelial growth factor levels in women with gestational diabetes mellitus and nondiabetic controls. *Gynecol. Obstet. Invest* **65:**227–232; 2008.
[43] Mazzanti, L.; Nanetti, L.; Vignini, A.; Rabini, R. A.; Grechi, G.; Cester, N.; Curzi, C. M.; Tranquilli, A. L. Gestational diabetes affects platelet behaviour through modified oxidative radical metabolism. *Diabet. Med* **21:**68–72; 2004.
[44] Rajdl, D.; Racek, J.; Steinerova, A.; Novotny, Z.; Stozicky, F.; Trefil, L.; Siala, K. Markers of oxidative stress in diabetic mothers and their infants during delivery. *Physiol. Res.* **54:**429–436; 2005.
[45] Biri, A.; Onan, A.; Devrim, E.; Babacan, F.; Kavutcu, M.; Durak, I. Oxidant status in maternal and cord plasma and placental tissue in gestational diabetes. *Placenta* **27:**327–332; 2006.
[46] Kamath, U.; Rao, G.; Raghothama, C.; Rai, L.; Rao, P. Erythrocyte indicators of oxidative stress in gestational diabetes. *Acta Paediatr.* **87:**676–679; 1998.
[47] Collet, J. F.; D'Souza, J. C.; Jakob, U.; Bardwell, J. C. Thioredoxin 2, an oxidative stress-induced protein, contains a high affinity zinc binding site. *J. Biol. Chem.* **278:**45325–45332; 2003.
[48] Prasad, A. S.; Bao, B.; Beck, F. W.; Kucuk, O.; Sarkar, F. H. Antioxidant effect of zinc in humans. *Free Radic. Biol. Med.* **37:**1182–1190; 2004.
[49] Vallee, B. L.; Falchuk, K. H. The biochemical basis of zinc physiology. *Physiol. Rev.* **73:**79–118; 1993.
[50] Wu, T.; Rifai, N.; Roberts 2nd L. J.; Willett, W. C.; Rimm, E. B. Stability of measurements of biomarkers of oxidative stress in blood over 36 hours. *Cancer Epidemiol. Biomarkers Prev* **13:**1399–1402; 2004.
[51] Ghosh, S.; Pulinilkunnil, T.; Yuen, G.; Kewalramani, G.; An, D.; Qi, D.; Abrahani, A.; Rodrigues, B. Cardiomyocyte apoptosis induced by short-term diabetes requires mitochondrial GSH depletion. *Am. J. Physiol. Heart Circ. Physiol* **289:**H768–H776; 2005.
[52] Sakamaki, H.; Akazawa, S.; Ishibashi, M.; Izumino, K.; Takino, H.; Yamasaki, H.; Yamaguchi, Y.; Goto, S.; Urata, Y.; Kondo, T.; Nagataki, S. Significance of glutathione-dependent antioxidant system in diabetes-induced embryonic malformations. *Diabetes* **48:**1138–1144; 1999.
[53] Kang, Y. J.; Chen, Y.; Yu, A.; Voss-McCowan, M.; Epstein, P. N. Overexpression of metallothionein in the heart of transgenic mice suppresses doxorubicin cardiotoxicity. *J. Clin. Invest.* **100:**1501–1506; 1997.
[54] Cohen, G. A.; Hobbs, A. J.; Fitch, R. M.; Zinner, M. J.; Chaudhuri, G.; Ignarro, L. J. Nitric oxide regulates endothelium-dependent vasodilator responses in rabbit hindquarters vascular bed in vivo. *Am. J. Physiol.* **271:**H133–H139; 1996.
[55] Taylor, C. G. Zinc the pancreas, and diabetes: insights from rodent studies and future directions. *Biometals* **18:**305–312; 2005.
[56] Cai, L.; Wang, J.; Li, Y.; Sun, X.; Wang, L.; Zhou, Z.; Kang, Y. J. Inhibition of superoxide generation and associated nitrosative damage is involved in metallothionein prevention of diabetic cardiomyopathy. *Diabetes* **54:** 1829–1837; 2005.
[57] Merten, K. E.; Jiang, Y.; Kang, Y. J. Zinc inhibits doxorubicin-activated calcineurin signal transduction pathway in H9c2 embryonic rat cardiac cells. *Exp. Biol. Med. (Maywood)* **232:**682–689; 2007.
[58] Merten, K. E.; Feng, W.; Zhang, L.; Pierce, W.; Cai, J.; Klein, J. B.; Kang, Y. J. Modulation of cytochrome C oxidase-va is possibly involved in metallothionein protection from doxorubicin cardiotoxicity. *J. Pharmacol. Exp. Ther.* **315:**1314–1319; 2005.
[59] Ynsa, M. D.; Ren, M. Q.; Rajendran, R.; Sidhapuriwala, J. N.; van Kan, J. A.; Bhatia, M.; Watt, F. Zinc mapping and density imaging of rabbit pancreas endocrine tissue sections using nuclear microscopy. *Microsc. Microanal.* **15:**345–352; 2009.
[60] Singh, R. B.; Niaz, M. A.; Rastogi, S. S.; Bajaj, S.; Gaoli, Z.; Shoumin, Z. Current zinc intake and risk of diabetes and coronary artery disease and factors associated with insulin resistance in rural and urban populations of North India. *J. Am. Coll. Nutr.* **17:**564–570; 1998.
[61] Chen, M. D.; Liou, S. J.; Lin, P. Y.; Yang, V. C.; Alexander, P. S.; Lin, W. H. Effects of zinc supplementation on the plasma glucose level and insulin activity in genetically obese (ob/ob) mice. *Biol. Trace Elem. Res.* **61:**303–311; 1998.
[62] Uriu-Hare, J. Y.; Stern, J. S.; Reaven, G. M.; Keen, C. L. The effect of maternal diabetes on trace element status and fetal development in the rat. *Diabetes* **34:**1031–1040; 1985.
[63] Eriksson, U. J. Diabetes in pregnancy: retarded fetal growth, congenital malformations and feto-maternal concentrations of zinc, copper and manganese in the rat. *J. Nutr* **114:**477–484; 1984.
[64] Uriu-Hare, J. Y.; Stern, J. S.; Keen, C. L. Influence of maternal dietary Zn intake on expression of diabetes-induced teratogenicity in rats. *Diabetes* **38:**1282–1290; 1989.
[65] Eriksson, U. J.; Borg, L. A. Protection by free oxygen radical scavenging enzymes against glucose-induced embryonic malformations in vitro. *Diabetologia* **34:**325–331; 1991.
[66] Eriksson, U. J.; Borg, L. A. Diabetes and embryonic malformations. Role of substrate-induced free-oxygen radical production for dysmorphogenesis in cultured rat embryos. *Diabetes* **42:**411–419; 1993.
[67] Eckel, R. H.; Wassef, M.; Chait, A.; Sobel, B.; Barrett, E.; King, G.; Lopes-Virella, M.; Reusch, J.; Ruderman, N.; Steiner, G.; Vlassara, H. Prevention Conference VI: Diabetes and Cardiovascular Disease: Writing Group II: pathogenesis of atherosclerosis in diabetes. *Circulation* **105:**e138-143; 2002.
[68] Liu, L.; Zhang, X. J.; Jiang, S. R.; Ding, Z. N.; Ding, G. X.; Huang, J.; Cheng, Y. L. Heat shock protein 27 regulates oxidative stress-induced apoptosis in cardiomyocytes: mechanisms via reactive oxygen species generation and Akt activation. *Chin. Med. J. (Peking)* **120:**2271–2277; 2007.
[69] Cai, L.; Li, W.; Wang, G.; Guo, L.; Jiang, Y.; Kang, Y. J. Hyperglycemia-induced apoptosis in mouse myocardium: mitochondrial cytochrome C-mediated caspase-3 activation pathway. *Diabetes* **51:**1938–1948; 2002.
[70] Hwang, J. T.; Kwon, D. Y.; Park, O. J.; Kim, M. S. Resveratrol protects ROS-induced cell death by activating AMPK in H9c2 cardiac muscle cells. *Genes Nutr* **2:**323–326; 2008.
[71] Kumar, S.; Sitasawad, S. L. *N*-Acetylcysteine prevents glucose/glucose oxidase-induced oxidative stress, mitochondrial damage and apoptosis in H9c2 cells. *Life Sci* **84:**328–336; 2009.
[72] Truong-Tran, A. Q.; Carter, J.; Ruffin, R. E.; Zalewski, P. D. The role of zinc in caspase activation and apoptotic cell death. *Biometals* **14:**315–330; 2001.